

NASA's Black Marble Nighttime Lights Product Suite

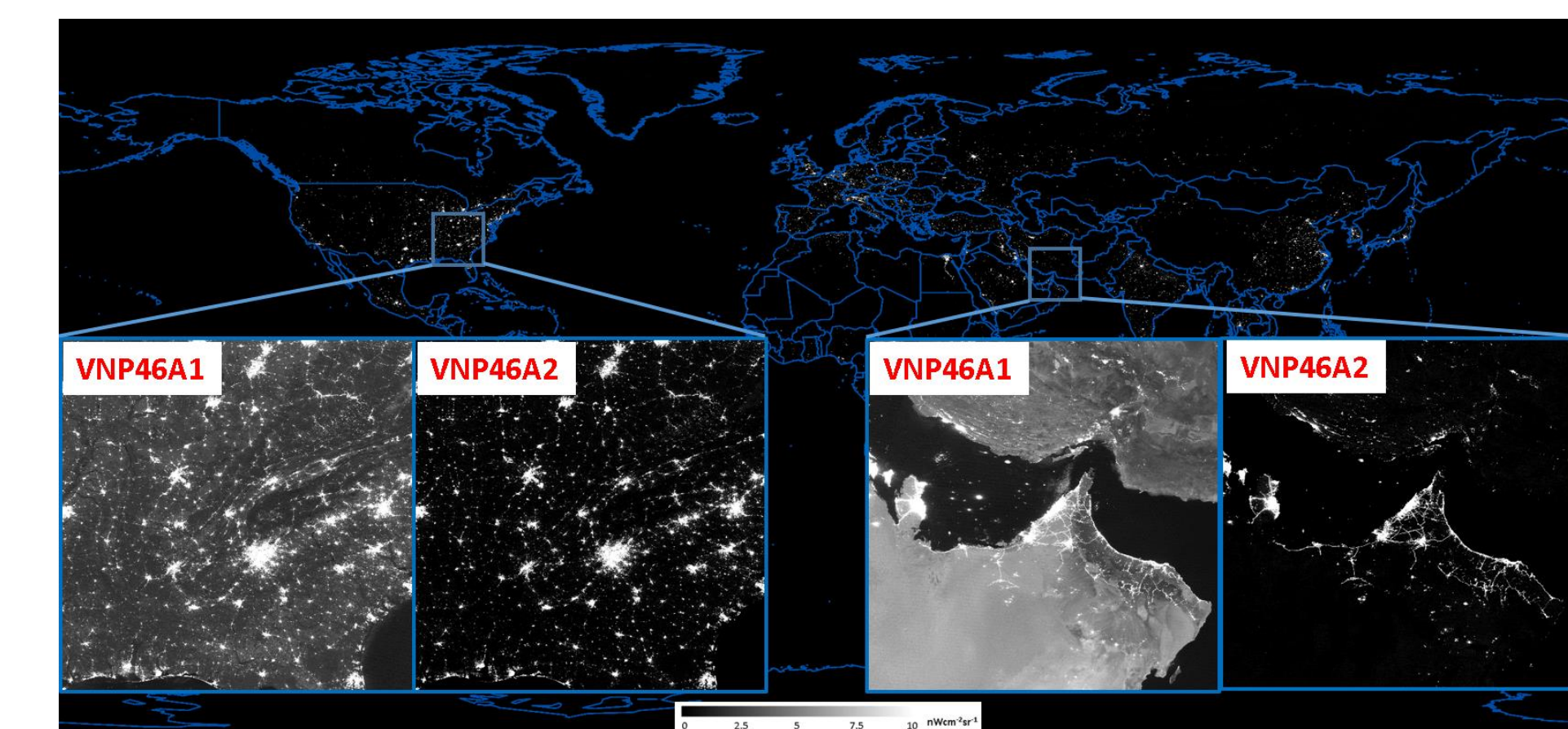
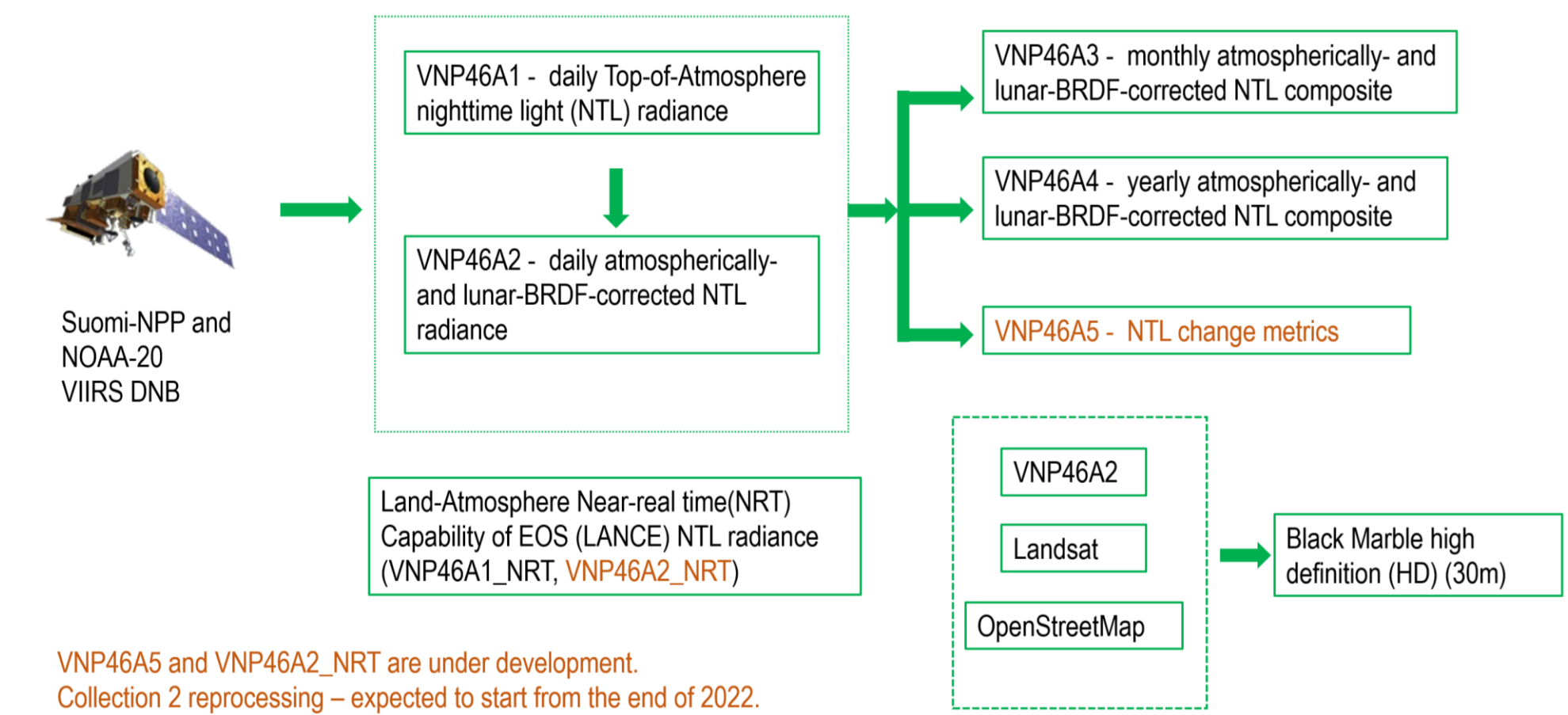
Miguel O. Román^{1,2}, Zhuosen Wang^{2,3}, Eleanor Stokes^{2,4}, Virginia Kalb²
Ranjay Shrestha^{2,5}, Srijia Chakraborty^{2,4}, and Ian Paynter^{1,2}



¹Leidos Civil Group, Reston, VA; ²NASA Goddard Space Flight Center, Greenbelt, MD; ³University of Maryland, College Park, MD;
⁴Universities Space Research Association, Columbia, MD; ⁵Science Systems and Applications, Inc., Lanham, MD 20706

Product Overview

NASA has developed a global suite of standard products that represent the current state-of-the-art in nighttime lights (NTL) applications. NASA's Black Marble nighttime lights product suite (VNP46). Distributed in Level 3 format, NASA's Black Marble products have been available from January 2012-present with data from the Visible Infrared Imaging Radiometer Suite (VIIRS) Day/Night Band (DNB), aboard the Suomi-NPP satellite, at 500m spatial resolution via NASA's Level-1 and Atmosphere Archive and Distribution System Distributed Active Archive Center (LAADS-DAAC).



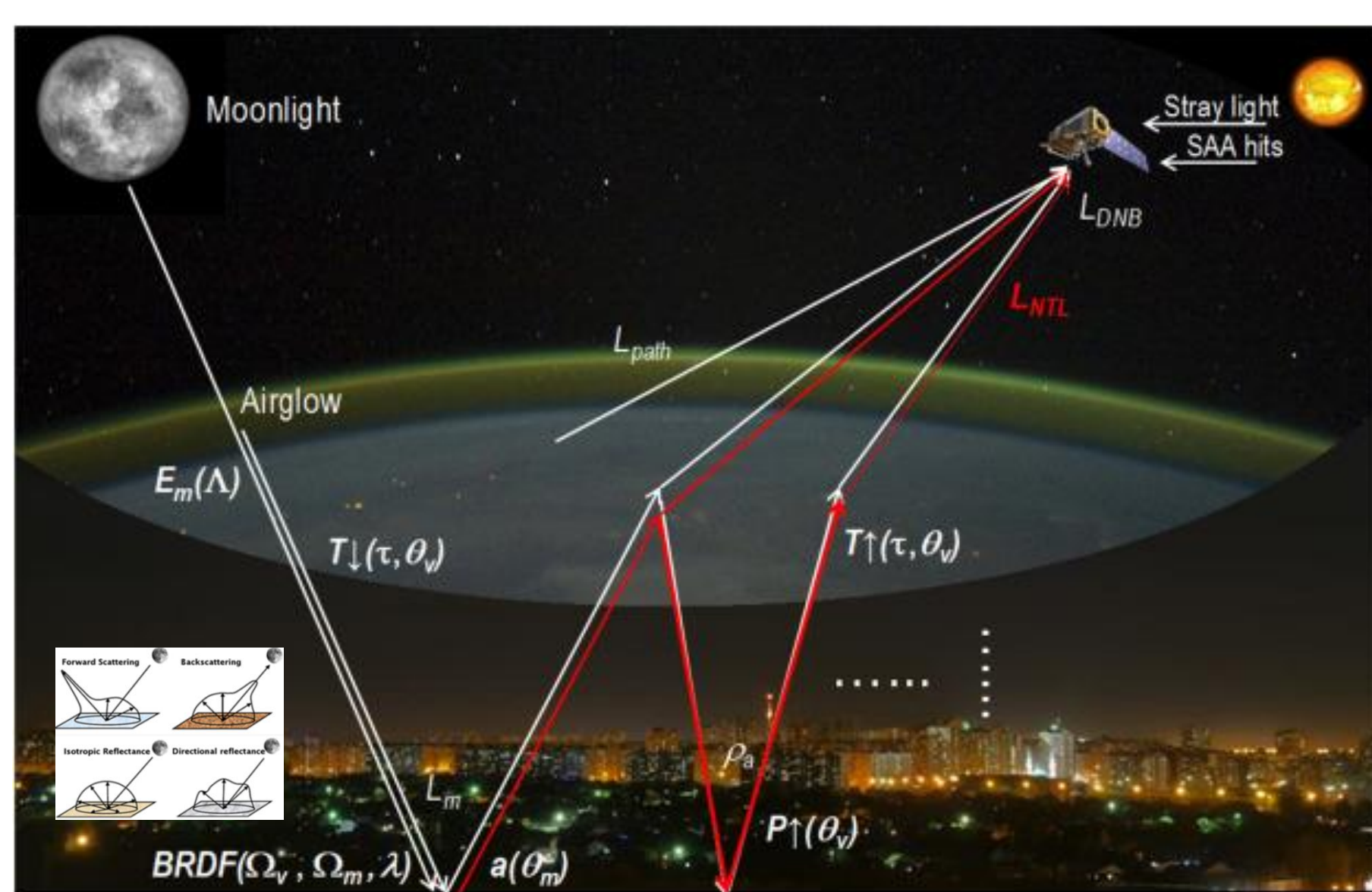
Black Marble Daily Top-of-Atmosphere (VNP46A1) and Lunar BRDF-corrected (VNP46A2) products.



Continental United States of NASA's Black Marble 2016 annual composite (VNP46A4).

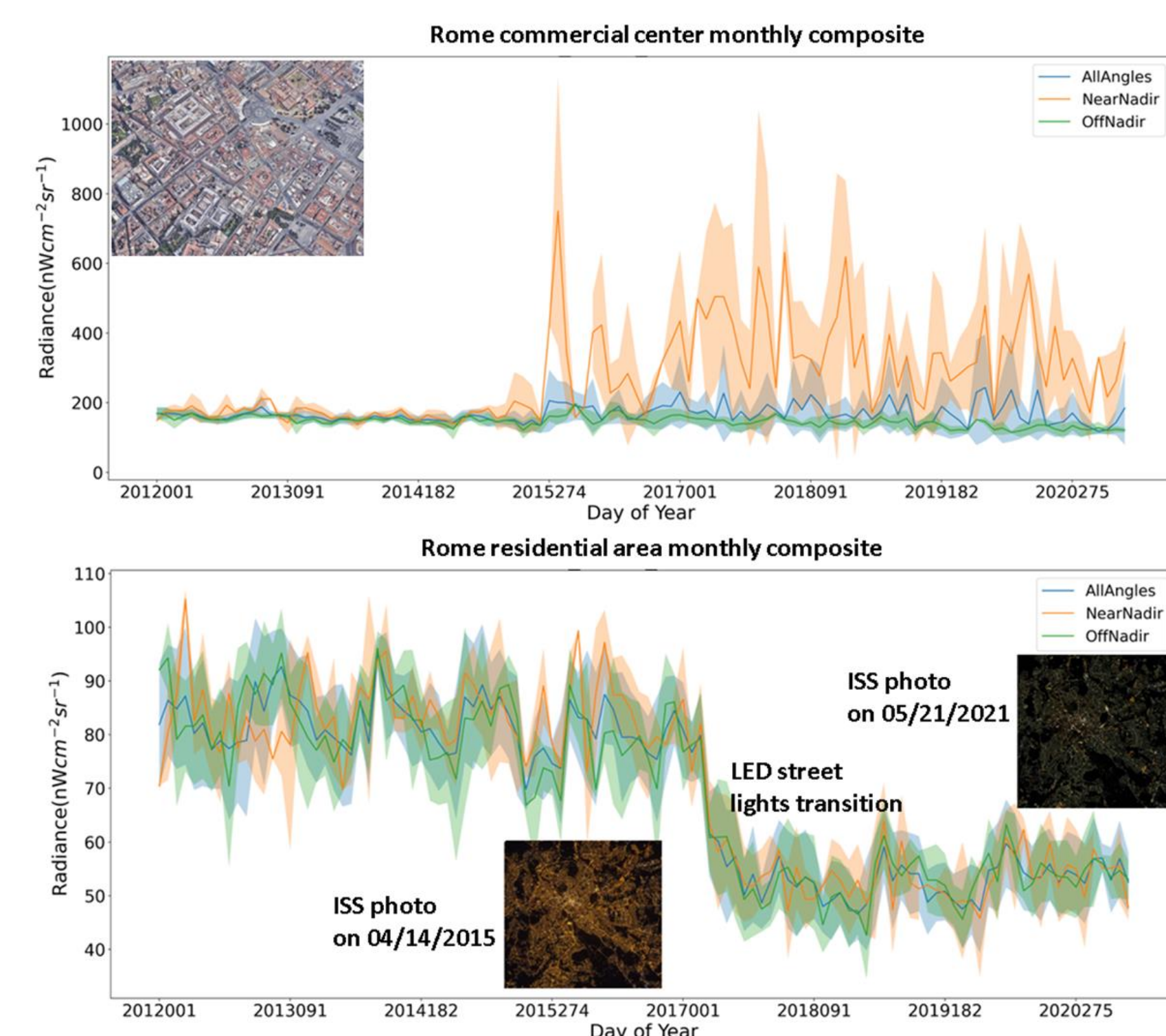
Overview of the Algorithm

The NASA Black Marble algorithm produces daily cloud-free nighttime radiances that have been corrected for atmospheric, terrain, lunar BRDF, and straylight effects. Key algorithm enhancements include: (1) lunar irradiance modeling to resolve non-linear changes in phase and libration; (2) vector radiative transfer and lunar bidirectional surface anisotropic reflectance modeling to correct for atmospheric and bidirectional reflectance distribution function (BRDF) effects; (3) geometric-optical and canopy radiative transfer modeling to account for seasonal variations in NTL; and (4) temporal gap-filling to reduce persistent data gaps.



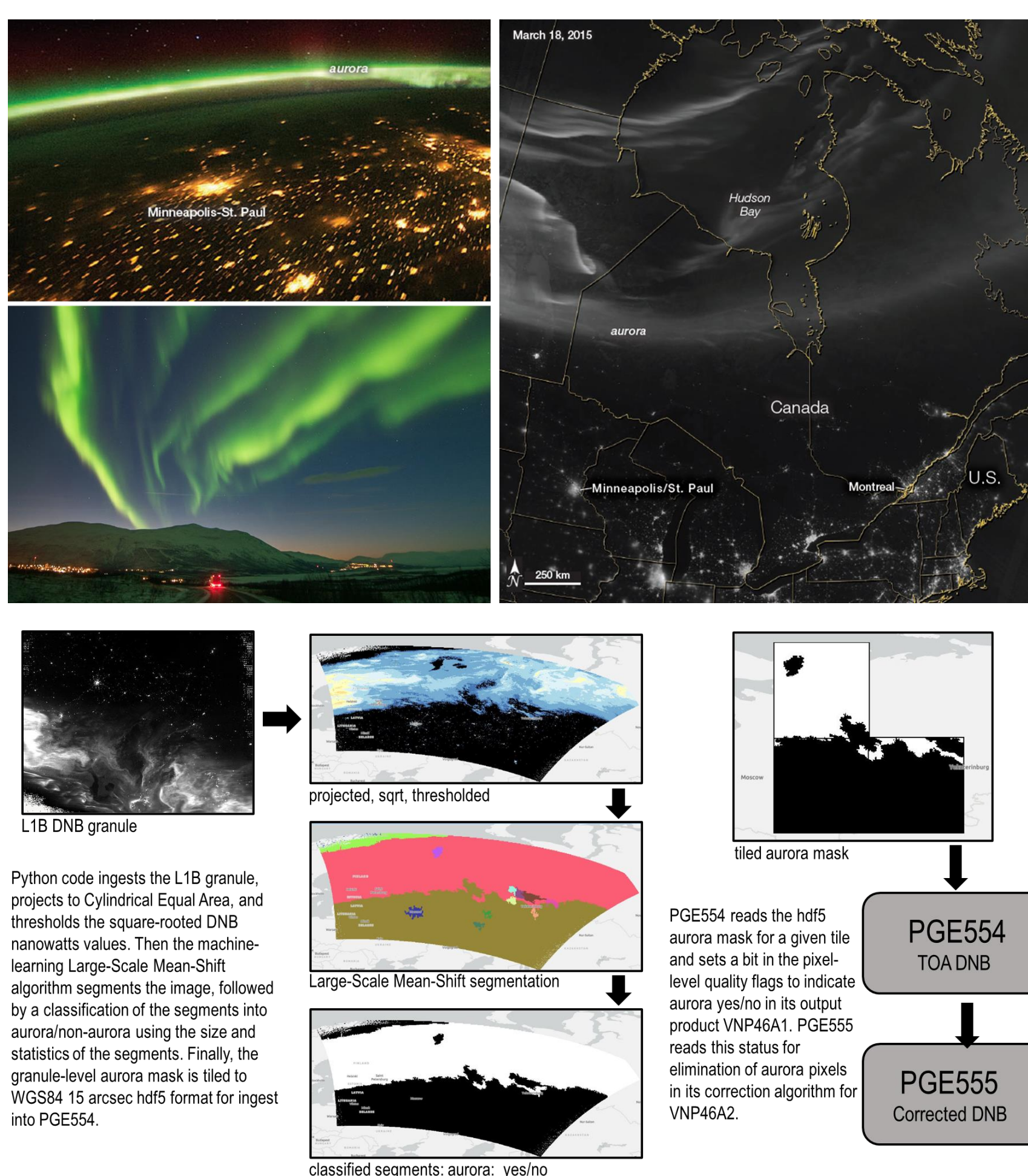
Overview of NASA's Black Marble retrieval strategy. During the ~50% portion of the lunar cycle when moonlight is present at the time of satellite observation, the surface upward radiance from artificial light emissions, L_{NL} [units of $nWatts \cdot cm^{-2} \cdot sr^{-1}$], can be extracted from at-sensor nighttime radiance at TOA (L_{DNB}). L_{path} is the nighttime path radiance, $a(\theta_s)$ is the VIIRS-derived actual surface albedo. The atmospheric backscatter is given by p_a . $T_1(\tau, \theta_s)$ and $T_2(\tau, \theta_s)$ are the total transmittances along the lunar-ground and ground-sensor paths (respectively). $P_1(\theta_s)$ is the probability of the upward transmission of NTL emissions through the urban vegetation canopy.

Multi-Angle Nighttime Lights Products



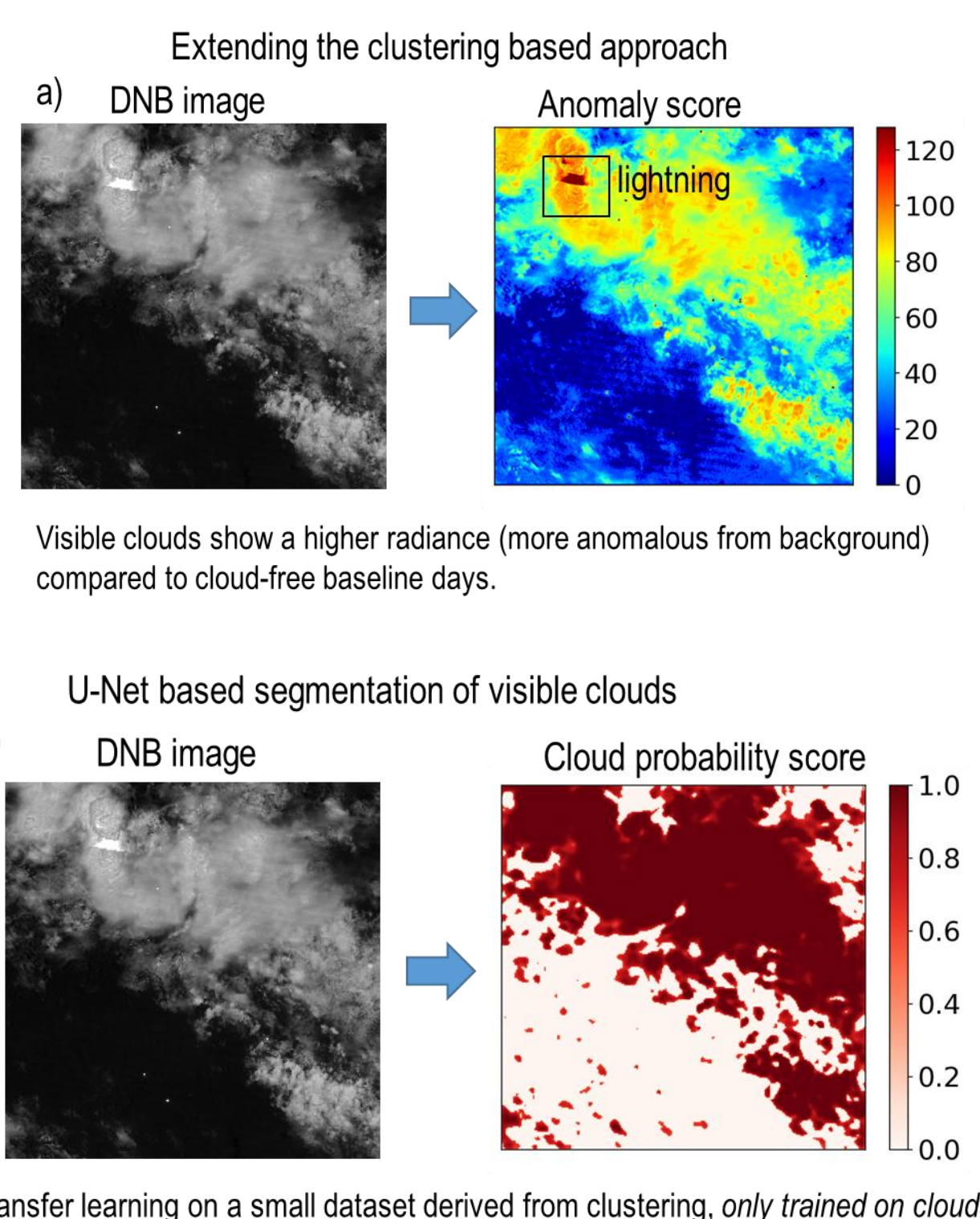
Black Marble monthly products (VNP46A3) with multiple view angle categories.

Aurora Detection



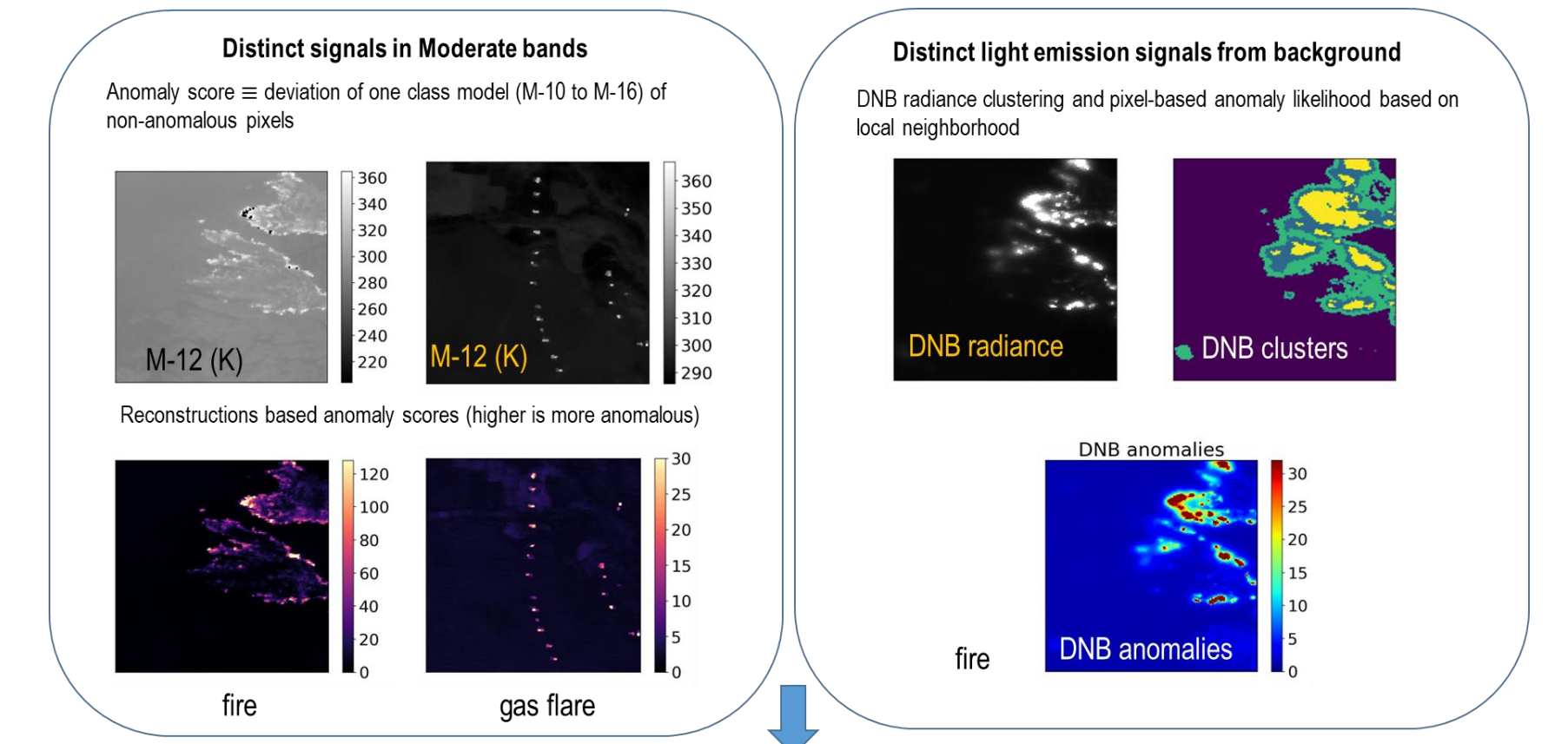
Defining an Aurora Mask from VIIRS Level-1B Day/Night Band and Daily Black Marble Products.

Nighttime Cloud Detection

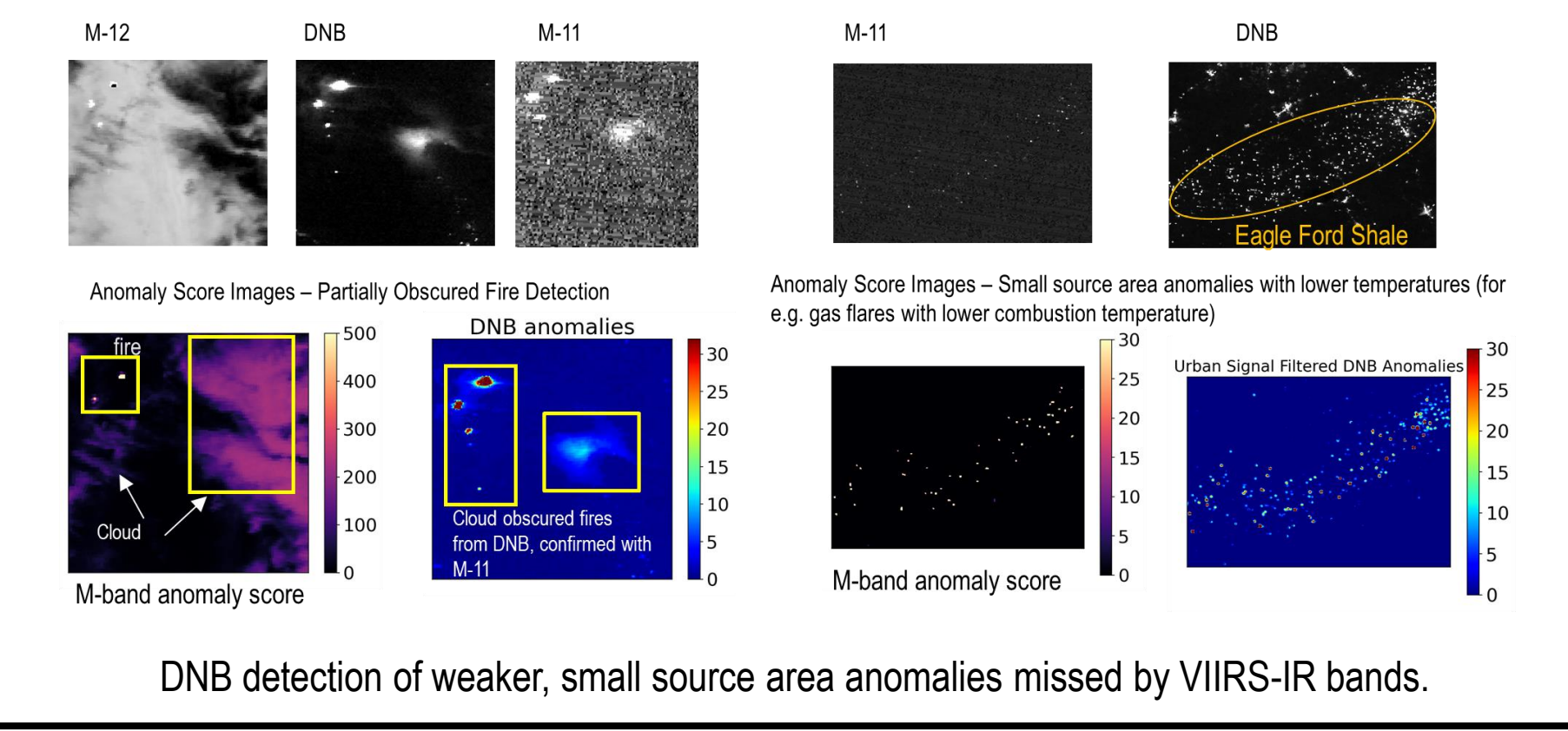


AI/ML is used to improve the detection of thin clouds that may not have a distinct thermal signature. The unsupervised method naturally outlines varying radiance classes (16-line signature of lightning) and generates a catalog for different DNB features (e.g., cloud, smoke, lightning). Examining segmentation methods such as U-net and fully connected networks to outline cloud pixels. Future improvement: improve model performance by expanding the training set, outlining multiple classes, and integrating with VIIRS nighttime-IR bands.

Thermal Anomaly Detection

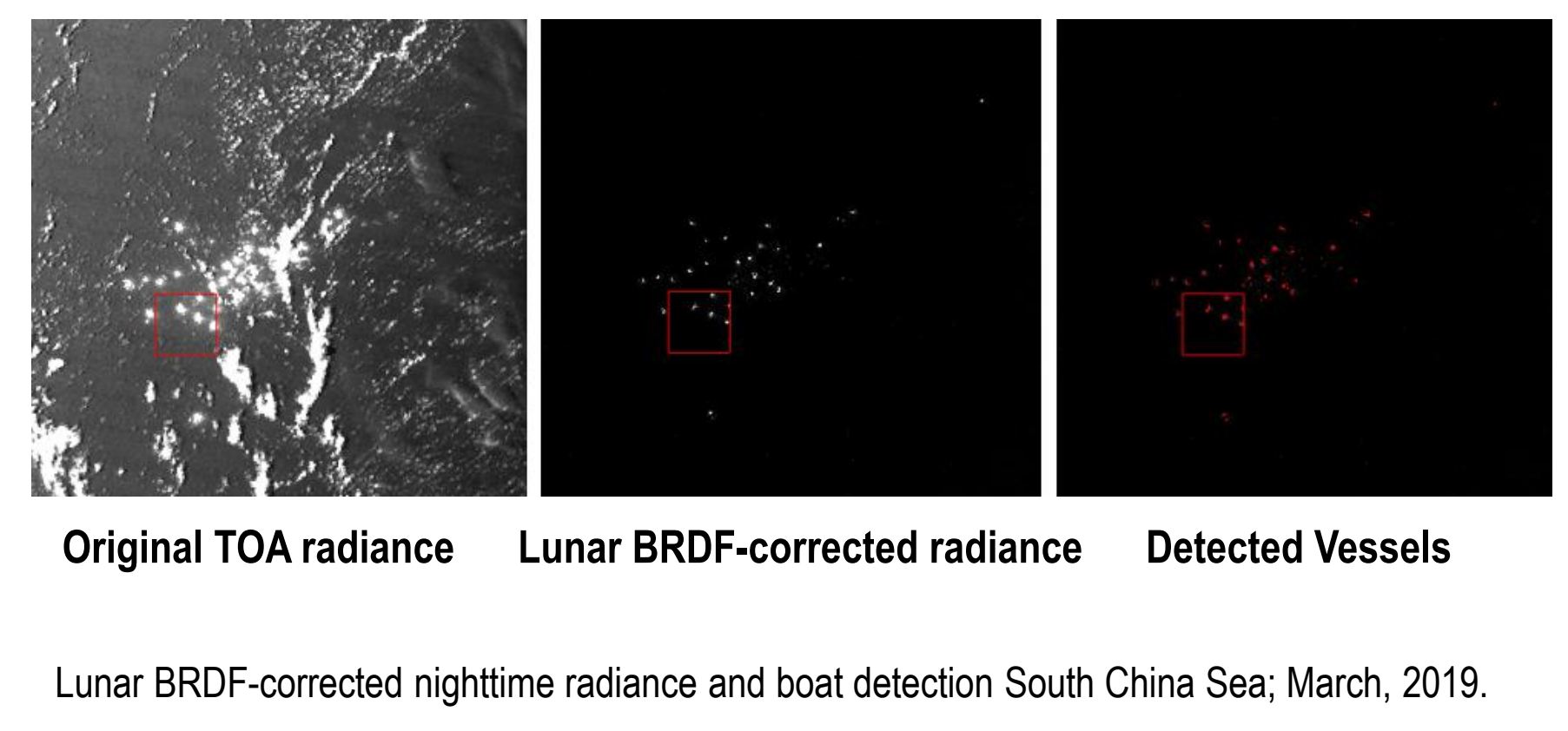


Joint multispectral normal class model to detect thermal and light emission signal of anomalies. Implemented unsupervised approach that learns background model to detect deviations. Detected anomaly consists of both thermal and light emission signals. M-band model is derived from autoencoder, pca, reed-xiao detectors, etc. DNB detection is based on clustering the scene and expressing each pixel as a function of its neighbors based on cluster properties. High radiance pixels after removing urban signal, electric lightning are anomalies. These are further filtered to retain pixels that show positive deviation (2 sigma away from background) in at least one M-band.



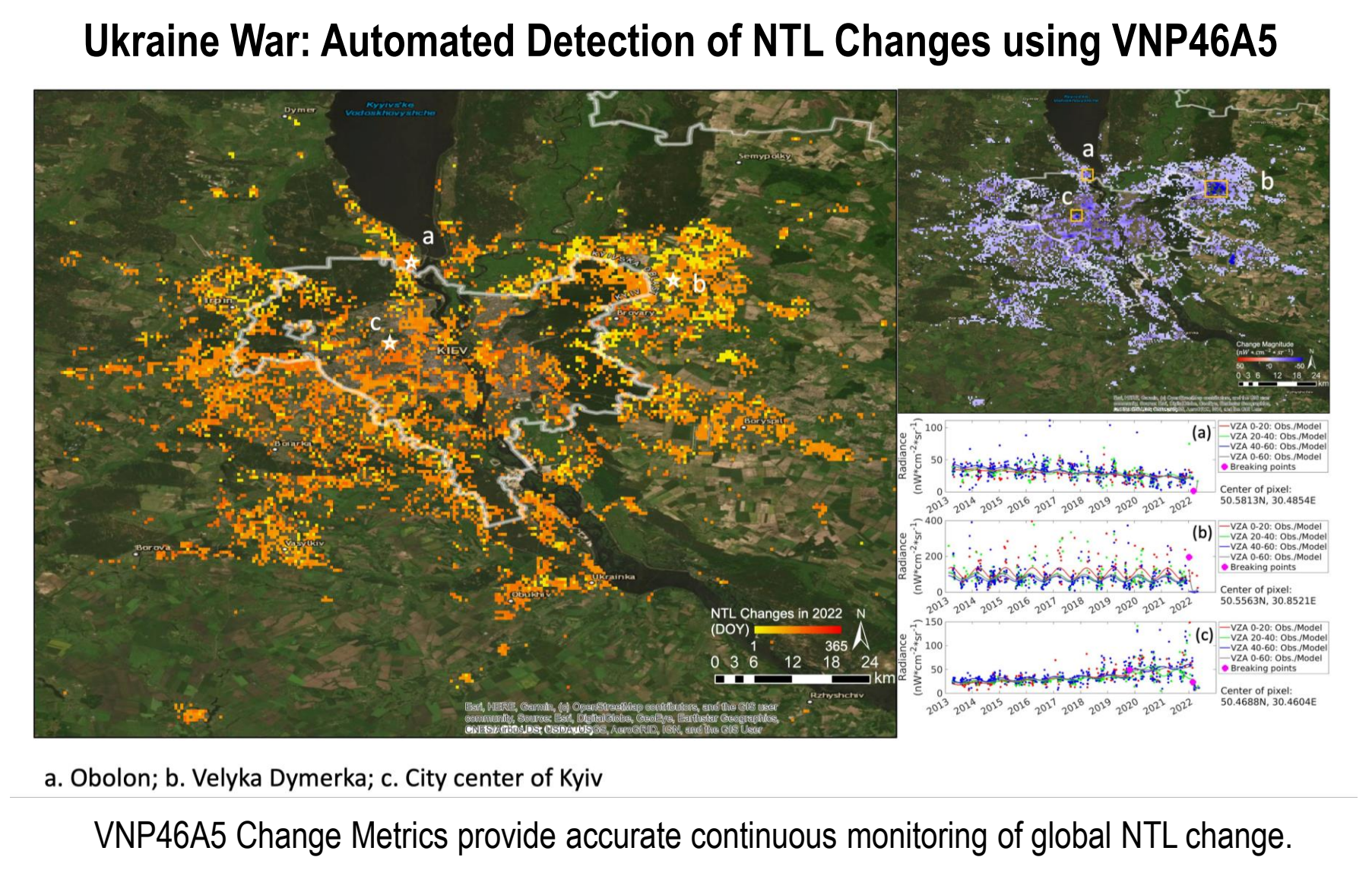
DNB detection of weaker, small source area anomalies missed by VIIRS-IR bands.

Nighttime Vessel Detection



Lunar BRDF-corrected nighttime radiance and boat detection South China Sea; March, 2019.

Conflict and Population Displacement



VNP46A5 Change Metrics provide accurate continuous monitoring of global NTL change.

References

Li, T., Zhu, Z., Wang, Z., Román, M.O., Kalb, V.L. and Zhao, Y., 2022. Continuous monitoring of nighttime light changes based on daily NASA's Black Marble product suite. Remote Sensing of Environment, 282, p.113269. doi:10.1016/j.rse.2022.113269
Wang, Z., Shrestha, R.M., Román, M.O. and Kalb, V.L., 2022. NASA's Black Marble Multi-Angle Nighttime Lights Temporal Composites. IEEE Geoscience and Remote Sensing Letters. doi: 10.1109/LGRS.2022.3176616.
Zhang, J., Reid, J.S., Miller, S.D., Román, M., Wang, Z., Spurr, R.J. and Jaker, S., 2022. Sensitivity studies of nighttime TOA radiances from artificial light sources using a 3-D radiative transfer model for nighttime aerosol retrievals. Atmospheric Measurement Techniques Discussions, pp.1-28. doi:10.5194/amt-2022-232.
Román, M.O., Stokes, E.C., Shrestha, R., Wang, Z., Schultz, L., Sepúlveda Carlo, E.A., Sun, Q., Bell, J., Molthan, A., Kalb, V., Ji, C., Seto, K.C., McClain, S.N., and Enekel, M. (2019). Satellite-based assessment of electricity restoration efforts in Puerto Rico after Hurricane Maria. PLoS ONE 14 (6). doi:10.1371/journal.pone.0218883.
Román, M.O., Wang, Z., Sun, Q., Kalb, V., Miller, S.D., Molthan, A., Schultz, L., Bell, J., Stokes, E.C., Pandey, B. and Seto, K.C., et al. (2018). NASA's Black Marble nighttime lights product suite. Remote Sens. Environ. 210, 113-143. doi:10.1016/j.rse.2018.03.017.
Román, M.O. and Stokes, E.C. (2015). Holidays in lights: Tracking cultural patterns in demand for energy services. Earth's Future, 3, 182-205.

Acknowledgements

This work was supported by NASA's Terra, Aqua, Suomi-NPP, and NOAA-20 program grant 80NSSC22K0199, NASA's Remote Sensing Theory for Earth Science program grant 80NSSC20K1748, and the Office of the Director of National Intelligence (ODNI), Intelligence Advanced Research Projects Activity (IARPA), via 2021-2011000005. The views and conclusions contained herein are those of the authors and should not be interpreted as necessarily representing the official policies, either expressed or implied, of ODNI, IARPA, or the U.S. Government. The U.S. Government is authorized to reproduce and distribute reprints for governmental purposes notwithstanding any copyright annotation therein.